Theoretical Study of Thermal Decomposition Mechanism of Oxalic Acid

James Higgins, Xuefeng Zhou, Ruifeng Liu,* and Thomas T.-S. Huang*

Department of Chemistry, East Tennessee State University, Johnson City, Tennessee 376140-0695

Received: November 15, 1996; In Final Form: January 17, 1997[⊗]

Density functional theory B3LYP/6-31G** and ab initio MP2/6-31G** and MP4(SDQ)/6−311++G** calculations were carried out to study the structures and isomerization and decomposition mechanisms of oxalic acid. The B3LYP structures and relative energies of the rotational isomers of oxalic acid are found very similar to MP2 results, confirming that the most stable isomer is the doubly intramolecular hydrogen-bonded C_{2h} structure **E1**, with four other planar isomers within 6 kcal/mol. It is predicted that unimolecular formation of carbon dioxide and dihydroxycarbene (DHC) from oxalic acid has an activation barrier of 31 kcal/mol and that unimolecular formation of HCOOH from DHC has an activation barrier about 31 kcal/mol higher. The unimolecular formation of CO_2, CO and H_2O from oxalic acid via a concerted transition state has an activation barrier of only 42 kcal/mol, indicating it is a more favorable unimolecular decomposition channel. On the other hand, hydrogen migration from oxygen to carbon of DHC to produce HCOOH can be accomplished through a hydrogen exchange with H_2O (a model for oxalic acid) with an activation barrier of less than 37 kcal/mol. Transition state theory calculations indicate that this bimolecular channel might be responsible for the rapid formation of CO_2 and HCOOH in gas phase oxalic acid thermal decomposition, thus confirming the proposal of Bock and Redington. With increasing temperature the unimolecular channel to produce CO_2, CO, and H_2O might become significant.

1. Introduction

There have been many experimental[1−6] and several theoretical[6−8] studies of thermal decomposition of oxalic acid. The experimental studies[2] firmly established that the major decomposition products of oxalic acid vapor over the temperature range 400−430 K are equimolar quantities of carbon dioxide and formic acid. On the other hand, major products of 257−313 nm photolysis of oxalic acid vapor were found[4,5] to be CO_2, HCOOH, CO, and H_2O. The photolysis results were explained[4] by two primary decomposition channels producing CO_2 + HCOOH and CO_2 + CO + H_2O, respectively, with the first channel about 2.6 times faster. These results were, however, not supported by a detailed ab initio study[5] at the MP2/4-31G//HF/3-21G level, which concluded that the unimolecular channel leading to the formation of CO_2 + CO + H_2O has the lowest activation barrier, while unimolecular channels leading to the formation of CO_2 and HCOOH have activation barriers at least 35 kcal/mol higher. The discrepancy between the experimental and theoretical results might be due to several factors. The theoretical methods used in the previous studies may not be sufficiently reliable or there may be other important reaction routes not considered, or a significant fraction of oxalic acids may decompose at the walls of the container before the gas is analyzed.

To reconcile the experimental and theoretical results and gain a better understanding of the mechanisms and kinetics of gas phase decomposition of oxalic acid, we carried out a detailed theoretical study, at a higher level of theory, of the isomerization and decomposition channels. The reaction routes studied are described below.

Rotational Isomers and Isomerization Pathways. Rotational isomerization of oxalic acid was the subject of a detailed ab initio study[6] at MP2/6-31G** level of theory. Six rotational isomers were identified, and activation barriers of some conceivable isomerization processes were obtained. In the present study, we calculated the structures, energies, and vibrational frequencies of these isomers and isomerization processes by density functional theory using Becke's three-parameter hybrid DFT/HF method[9] with Lee−Yang−Parr's correlation functional[10] (B3LYP) and the 6-31G** basis set. The results are compared with those obtained from the much more expensive MP2/6-31G** calculations. It is found that the B3LYP results are in good agreement with those of MP2. Therefore, B3LYP/6-31G** was also used in the present study to determine the equilibrium and transition state structures of the thermal decomposition processes. The rotational isomers and conceivable pathways connecting them are shown in Scheme 1. **E1** through **E6** are equilibrium structures which are connected by internal rotation around the C−O or C−C bonds.

Decomposition Channels. Scheme 2 summarizes the decomposition channels of oxalic acid proposed in previous experimental and theoretical studies. Channel 2a was proposed by Lapidus et al.[2] to explain the formation of CO_2 and HCOOH with a low preexponential factor. Channel 2b was proposed by Yamamoto and Back[4] who suggested that the energy required to form dihydroxycarbene (DHC) makes channel 2a unlikely. The theoretical study of Kakumoto et al.[5] at MP2/3-21G//HF/3-21G level found that channel 2b has an activation barrier of 71.4 kcal/mol, while the formation of DHC has an activation energy of only 31.2 kcal/mol. However, unimolecular hydrogen migration from oxygen to carbon in DHC to produce formic acid was found to have an activation energy of 67.4 kcal/mol. They investigated channel 2c and found this channel has an activation barrier of only 23.7 kcal/mol at MP2/3-21G//HF/3-21G level, and 28.3 kcal/mol at MP2/4-31G//HF/4-31G level of theory. However, these results cannot explain the major products (CO_2 and HCOOH) observed[2] in the vapor phase thermal decomposition of oxalic acid.

To explain the fact that CO_2 and HCOOH are major products of thermal decomposition of oxalic acid vapor, Bock and Redington[8] suggested that a bimolecular process such as Scheme 2d might be responsible for fast formation of HCOOH from

[⊗] Abstract published in *Advance ACS Abstracts,* March 1, 1997.

S1089-5639(96)03819-4 CCC: $14.00

SCHEME 1. Rotational isomerization mechanism of oxalic acid, numbers in parentheses are relative energies (in kcal/mol) calculated by B3LYP/6-31G plus zero-point vibrational energy.**

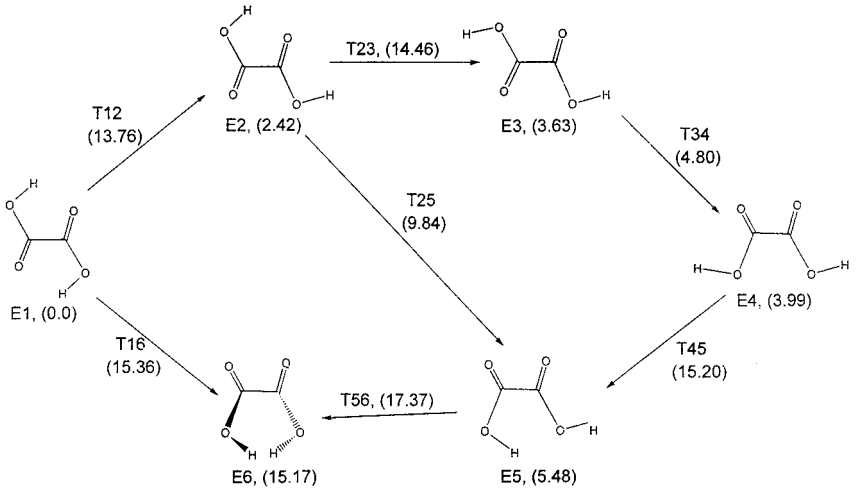

DHC. However, no theoretical studies have been carried out to investigate feasibility of this proposal.

To better understand the mechanisms of the decomposition reaction, we optimized all the intermediate and transition states of the unimolecular channels in Scheme 2a−c. In addition, we also investigated the feasibility of Scheme 2d by using a H_2O molecule in the place of oxalic acid, because it is a smaller model and therefore easier to handle computationally. H_2O is also a product of channel 2c which might be the most favorable unimolecular channel.

2. Computational Details

All quantum mechanical calculations were carried out using Gaussian 94 program package.[11] The equilibrium and transition state structures were fully optimized by B3LYP/6-31G**. Vibrational analyses were carried out, at the same level of theory, to characterize the optimized structures as equilibrium or transition states. Intrinsic reaction coordinate (IRC) analysis[12] was carried out for each decomposition transition state to make sure that it is the transition structure connecting the desired reactants and products. Relative energies were calculated at the B3LYP/6-31G** structures by B3LYP/6−311++G**, MP4(SDQ)(FC)/6-31G**, and MP4(SDQ)(FC)/6−311++G**. Zero-point vibrational energies (ZPE) were taken into account and approximated by one-half of the sum of B3LYP/6-31G** harmonic frequencies. The B3LYP/6-31G** harmonic frequencies were also used to evaluate activation enthalpies and activation entropies which were required for evaluating rate constants of probable decomposition channels by transition state theory.[13]

3. Results and Discussions

3.1. Structures and Relative Energies of Rotational Isomers. The optimized B3LYP/6-31G** equilibrium structures of the rotational isomers and their relatives energies are compared with ab initio MP2/6-31G** results[6] and available gas phase electron diffraction data[14] in Figure 1. In this figure, bond lengths are given in Å, angles in degrees, and relative energies in kcal/mol. Relative energies are given as the numbers following the name of each structure. The first entry is result of B3LYP/6-31G**; the second entry is result of MP2/6-31G**. It is shown that structural parameters calculated by MP2 and B3LYP are very similar, the largest difference in bond lengths is less than 0.01 Å, and the largest difference in bond angle is less than 1°. Both methods predict that the most stable isomer is **E1** followed by **E2**, **E3**, **E4**, **E5**, and **E6**. Isomers **E1**−**E5**

SCHEME 2. Decomposition mechanism of oxalic acid proposed in literature. (a)−(c) are unimolecular processes and (d) is a bimolecular process.

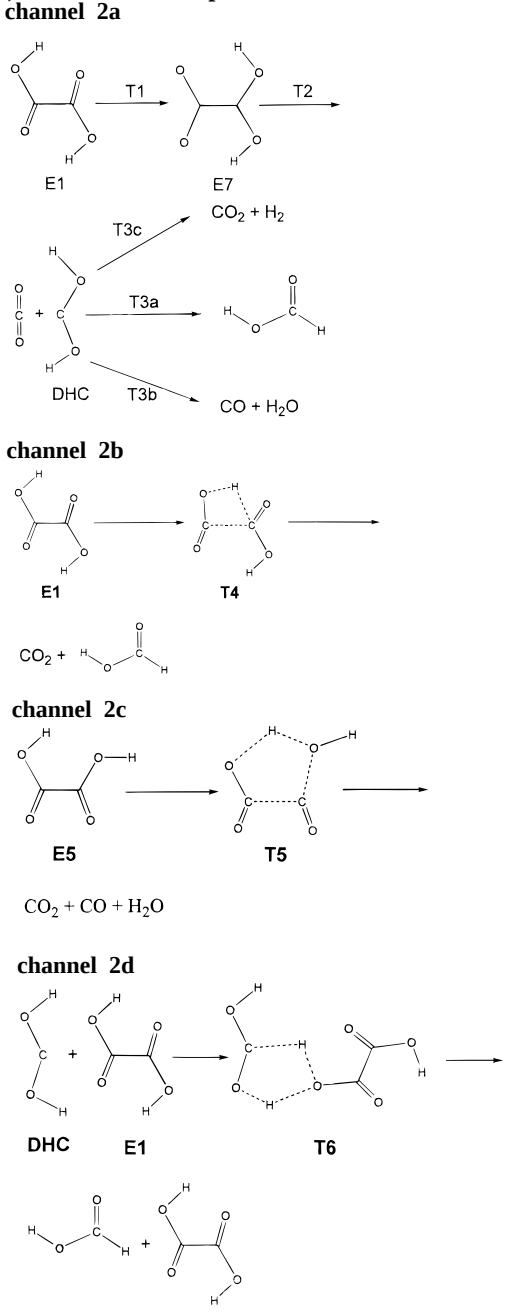

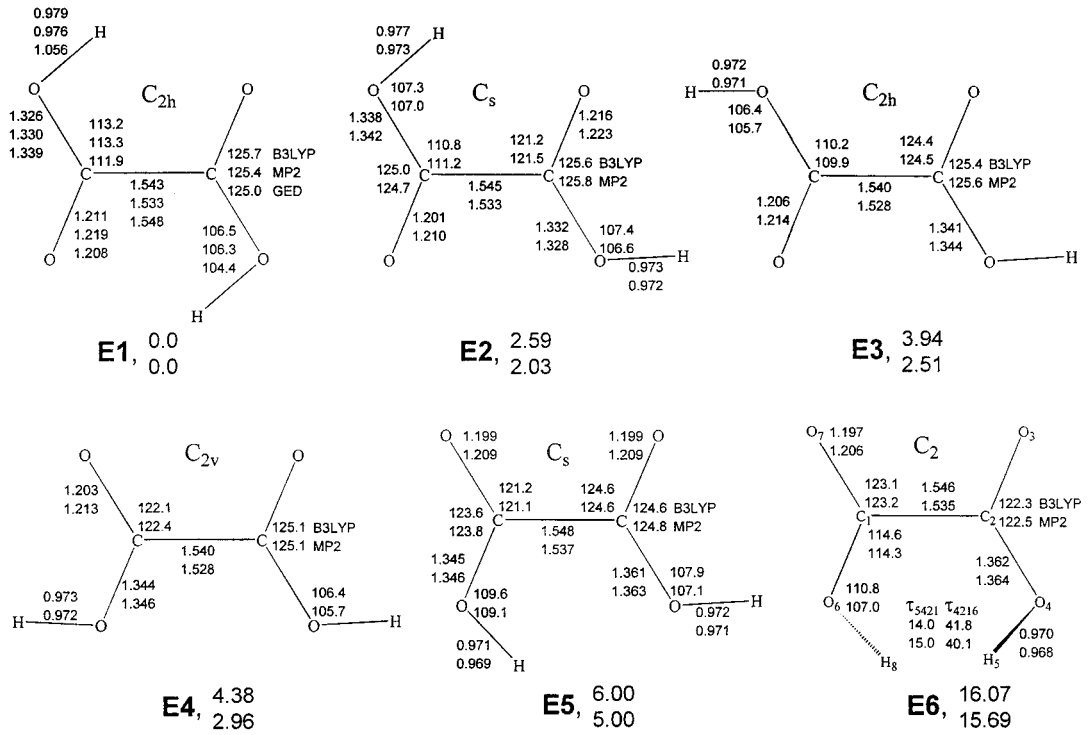

Figure 1. Calculated structural parameters (bond lengths in Å and angles in degrees) and relative energies (in kcal/mol, first entry is B3LYP result and second entry is MP2 result) of oxalic acid rotational isomers.

are very close in energy (within 6 kcal/mol). There was some controversy about which is the most stable structure. The electron diffraction study[14] found that the observed intensity pattern could be reasonably fit by both structures **E1** and **E3**, but **E1** was chosen on the basis of the observed low OH stretching frequency which suggests intramolecular hydrogen bonding.[14,15] Theoretical calculations gave, however, contradictory results. An early Hartree−Fock (HF) 6-31G study[8] found **E3** is more stable than **E1** by 0.5 kcal/mol, but HF/6-31G** and MP2/6-31G*//HF/6-31G calculations predict **E1** is more stable than **E3** by ca. 2 kcal/mol. On the other hand, MP2/4-31G//HF/4-31G calculations[5] indicated that **E3** is 0.8 kcal/mol more stable than **E1**, while MP2/3-21G//HF/3-21G calculations predicted **E1** is 0.9 kcal/mol more stable than **E3**. In these calculations, the structures were optimized only at the HF level of theory, therefore the results may be unreliable because the energy difference is so small. Our B3LYP/6-31G** results are in good agreement with results of the detailed MP2/6-31G**//MP2/6-31G** calculations,[6] predicting **E1** is the most stable followed by **E2** and **E3**. On the basis of the B3LYP/6-31G** energies and assuming Boltzmann distributions, the relative abundance of **E1**, **E2**, and **E3** at room temperature (298 K) is 1:0.013:0.0013. Relative abundance based on MP2/6-31G** energies is 1:0.032:0.014. Experimentally, IR signals of **E1** and **E2** were observed in a matrix isolation study.[6] Thus, the calculated results are in line with the matrix IR results.

A recent comprehensive study[16] of the performance of many theoretical methods in predicting fundamental vibrational frequencies concludes that the B3LYP/6-31G* harmonic frequencies are systematically higher than the observed fundamental frequencies, but after scaled by 0.9614, the calculated frequencies are in good agreement with the observed results. To assist spectroscopic identification of oxalic acid isomers, we have scaled the B3LYP/6-31G** frequencies of **E1**−**E6** by 0.9614; the scaled frequencies and corresponding B3LYP/6-31G** IR intensities are presented in Table 1. Available observed frequencies of **E1** and **E2** are also given in this table. Mean deviation between the calculated and observed frequencies of non-OH stretching modes is 16 cm^{-1}.

3.2. Structures and Relative Energies of Rotational Transition States. The optimized B3LYP/6-31G** transition structures connecting the rotational isomers of oxalic acid are presented in Figure 2. In this figure, the numbers in parentheses are relative energies (compared to the most stable isomer **E1**) in kcal/mol. It is shown by both the calculated C−C bond lengths and relative energies that both the equilibrium and rotational transition structures have almost pure C−C single bonds. Internal rotation around the C−C bond has the smallest barrier at **T34** (only 5.4 kcal/mol). Internal rotations around the C−O bond have significantly higher barriers, suggesting the singly occupied p orbital on carbon overlaps more effectively with the lone pair orbitals on oxygen than with the singly occupied p orbital on the other carbon. Relative energies of the equilibrium structures and transition states connecting them calculated by B3LYP/6-31G** plus ZPE are presented in the parentheses in Scheme 1. It is shown that, although **E2** is only 2.42 kcal/mol higher in energy than **E1**, they are separated by a rotational barrier of 13.76 kcal/mol. The lowest isomerization pathway for **E2** is a rotation around the C−C bond (transition state **T25**) with a barrier of 9.84 kcal/mol to **E5**. **E1**, **E2**, and **E5** were suggested as the starting structures in oxalic decomposition to produce different products.

3.3. Transition States and Energies of Thermal Decomposition. The transition structures optimized by B3LYP/6-31G** for oxalic acid decomposition along the channels depicted in Scheme 2 are presented in Figure 3. All the transition structures have been confirmed by vibrational analysis followed by intrinsic reaction coordinate analysis to make sure that they are the transition states connecting the desired reactants and products. The relative energies (compared to the most stable isomer **E1**) calculated at different levels of theory are presented in Table 2 and schematically in Figure 4. As it is shown, the overall lowest energy unimolecular decomposition pathway is Scheme 2c. The bimolecular decomposition channel, Scheme 2a coupled with Scheme 2d, is even lower. Details of these channels are discussed below.

Starting from **E1** and following Scheme 2a, a transition state, **T1**, for hydrogen migration was located. This transition state

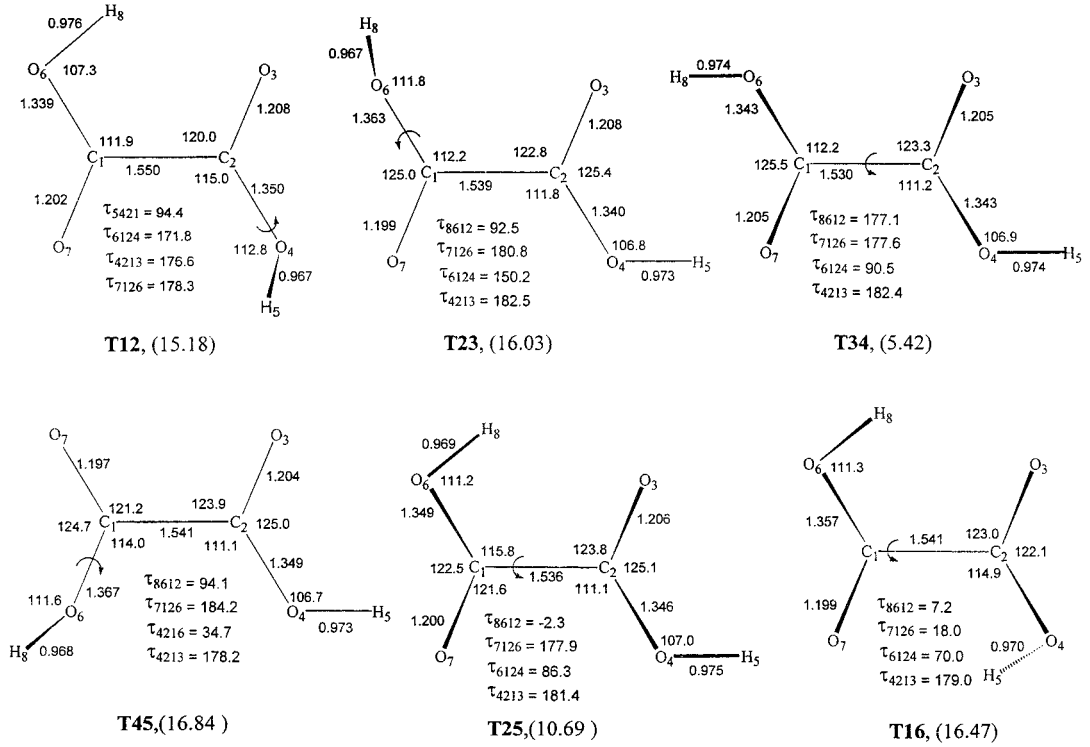

Figure 2. B3LYP/6-31G** structural parameters (bond lengths in Å and angles in degrees) and relative energies (in kcal/mol) of oxalic acid rotational transition states. Rotational isomerization mechanisms are depicted in Scheme 1.

TABLE 1: Observed[a] and Scaled[b] B3LYP/6-31G Frequencies of Oxalic Acid Isomers[c]**

E1			E2			E3		E4		E5		E6	
ν_{calc} (sym)	I_{IR}	ν_{obs}	ν_{calc} (sym)	I_{IR}	ν_{obs}	ν_{calc} (sym)	I_{IR}	ν_{calc} (sym)	I_{IR}	ν_{calc} (sym)	I_{IR}	ν_{calc} (sym)	I_{IR}
3500 (b_u)	233.45	3472	3602 (a′)	76.12	3576	3611 (b_u)	143.53	3600 (b_2)	112.49	3611 (a′)	38.06	3624 (b)	45.42
3497 (a_g)	0.0		3523 (a′)	111.72	3498	3611 (a_g)	0.0	3600 (a_1)	6.25	3605 (a′)	135.41	3624 (a)	59.82
1806 (b_u)	393.72	1817	1825 (a′)	220.74	1833	1790 (a_g)	0.0	1797 (a_1)	428.44	1825 (a′)	285.08	1836 (a)	240.19
1785 (a_g)	0.0	1800	1748 (a′)	246.06	1769	1780 (b_u)	509.21	1788 (b_2)	26.94	1812 (a′)	109.85	1814 (b)	137.04
1409 (a_g)	0.0	1423	1398 (a′)	38.97		1377 (a_g)	0.0	1379 (a_1)	56.54	1317 (a′)	324.99	1283 (a)	479.17
1301 (b_u)	854.78	1329	1302 (a′)	336.41	1322	1294 (b_u)	37.00	1269 (b_2)	29.23	1284 (a′)	181.82	1207 (b)	283.38
1190 (a_g)	0.0	1195	1169 (a′)	117.61	1217	1171 (a_g)	0.0	1140 (a_1)	356.81	1131 (a′)	24.51	1150 (a)	1.41
1180 (b_u)	8.53	1176	1140 (a′)	189.58	1141	1112 (b_u)	487.33	1132 (b_2)	164.06	1099 (a′)	227.54	1061 (b)	48.34
799 (a_g)	0.0	815	777 (a′)	23.76	798	785 (b_g)	0.0	785 (a_2)	0.0	766 (a″)	4.39	788 (a)	4.08
760 (b_g)	0.0		772 (a″)	11.24		762 (a_g)	0.0	760 (a_1)	10.58	758 (a′)	5.24	760 (a)	31.83
691 (a_u)	204.81	664	656 (a″)	32.03		662 (a_u)	273.70	676 (b_1)	272.02	626 (a′)	50.77	642 (b)	12.76
680 (b_g)	0.0		646 (a″)	226.33	650	615 (b_g)	0.0	619 (b_2)	82.75	618 (a″)	54.78	621 (b)	9.45
644 (b_u)	21.64		629 (a′)	47.64	622	612 (b_u)	135.94	605 (a_2)	0.0	536 (a″)	220.53	607 (a)	37.11
544 (a_g)	0.0		526 (a′)	9.98		508 (a_g)	0.0	491 (b_2)	4.69	509 (a′)	9.66	409 (b)	70.78
436 (a_u)	55.61	461	413 (a″)	1.75		410 (a_g)	0.0	414 (a_1)	9.10	413 (a′)	5.16	393 (b)	0.24
392 (a_g)	0.0	405	408 (a′)	16.61		401 (a_u)	12.39	400 (b_1)	13.35	403 (a″)	1.46	270 (a)	141.15
257 (b_u)	55.71	264	257 (a′)	14.93		253 (b_u)	5.74	258 (a_1)	1.04	269 (a′)	4.63	232 (a)	20.12
126 (a_u)	5.86		91 (a″)	4.45		33 (a_u)	3.92	20 (a_2)	0.0	60 (a″)	0.35	68 (a)	0.21

[a] IR active frequencies over 500 cm^{-1} were taken from ref 6; those below 500 cm^{-1} were taken from ref 15. Raman active frequencies were taken from ref 17. [b] Scale factor 0.9614 were taken from ref 16. [c] Structures of the isomers are given in Figure 1. The calculated IR intensities are given in km/mol.

is 25.5 kcal/mol higher than **E1** at MP4SDQ/6−311++G** level of theory and only 0.5 kcal/mol higher than the intermediate **E7**. However, after ZPE is taken into account, **T1** is slightly lower than **E7**, indicating that the transition state **T1** disappears when zero-point vibrational energy is taken into account. Starting from **E7**, the transition state for C−C cleavage, **T2**, is about 7 kcal/mol higher than **E7**, producing carbon dioxide (CO_2) and dihydroxycarbene (DHC). Thus, at the highest level of theory applied (MP4SDQ/6−311++G**//B3LYP/6-31G** plus ZPE), the production of CO_2 and DHC from **E1** is a concerted process via transition state **T2**, which has an activation barrier of 31 kcal/mol.

Another path for the production of CO_2 and DHC is to start from **E2**. It has been shown that **E1** and **E2** are separated by a barrier of only 13.78 kcal/mol, therefore both of them are present under thermal decomposition conditions. B3LYP/6-31G** transition state searches found only one transition structure, **T1a**, which is 35 kcal/mol higher in energy than **E1**. **T1a** is a transition state for concerted hydrogen migration and C−C bond cleavage. These results indicate that, unlike what was expected by Yamamoto and Back,[4] the formation of DHC from oxalic acid is a feasible thermal process. However, starting from DHC, unimolecular formation of HCOOH (via **T3a**), CO + H_2O (via **T3b**), or CO_2 + H_2 (via **T3c**) has energy barriers significantly higher than Scheme 2c and Scheme 2d. Compared to **E1**, the relative energies of **T3a** + CO_2, **T3b** + CO_2, and **T3c** + CO_2 are 62, 61, and 68 kcal/mol, respectively, thus making the unimolecular decomposition channel 2a a less favorable process than the formation of CO_2 + CO + H_2O via Scheme 2c (see discussions below).

Transition state searches for hydrogen migration from oxygen to carbon via Scheme 2b located a transition state for concerted

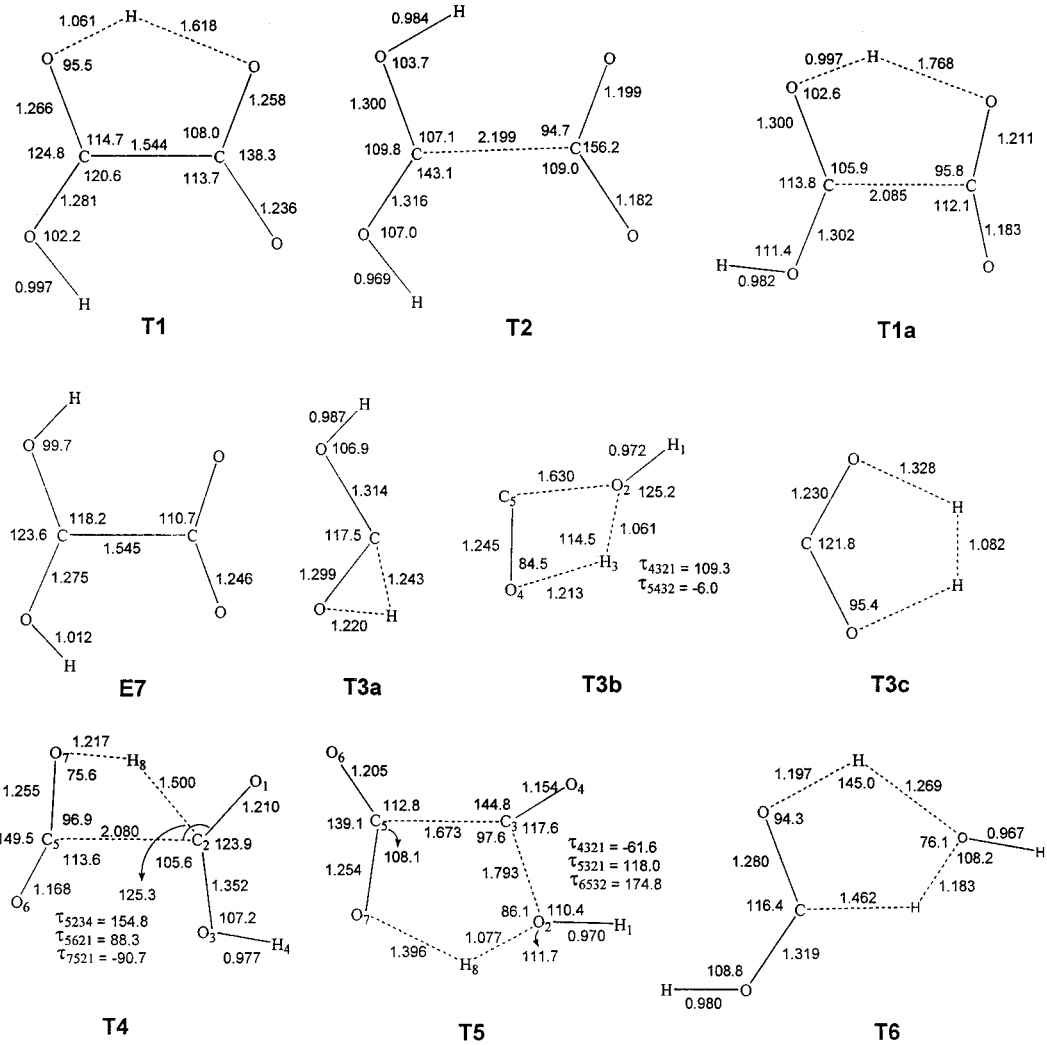

Figure 3. B3LYP/6-31G** structural parameters (bond lengths in Å and angles in degrees) of the transition states of oxalic acid decomposition. The decomposition mechanisms are depicted in Scheme 2; relative energies are presented in Table 1 and Figure 4.

TABLE 2: Energies[a] of Equilibrium and Transition Structures of Oxalic Acid Decomposition[b]

method	**E1**	**T1**	**E7**	**T2**	**T1a**	**T4**	**T5**	**T3a** + CO_2[c]	**T3b** + CO_2	**T3c** − CO_2	**T6** + CO_2 − H_2O[d]
6-31G**											
B3LYP	−378.33068	21.84	21.71	33.73	34.95	75.75	41.41	72.37	72.37	73.41	33.73
MP2	−377.34796	23.97	23.84	35.74	38.06	77.57	45.63	70.17	69.92	70.70	36.21
MP4SDQ	−377.36218	25.72	25.16	35.07	37.76	82.79	48.57	73.02	70.50	80.37	40.13
6-311++G**											
B3LYP	−378.45377	22.58	22.12	30.74	33.53	73.05	42.49	86.01	67.92	69.84	35.12
MP2	−377.54668	23.68	23.61	33.41	37.21	72.99	43.03	66.06	67.28	67.97	36.96
MP4SDQ	−377.55391	25.54	25.03	32.82	36.92	78.34	46.11	69.19	68.01	77.45	40.61
ZPE (kcal/mol)[e]	31.22	29.54	30.33	29.49	29.16	25.65	27.00	24.35	23.76	22.07	27.48
MP4SDQ+ZPE[f]		23.86	24.14	31.09	34.86	72.77	41.89	62.32	60.55	68.30	36.87

[a] Relative energies with respect to **E1** in kcal/mol. For **E1**, the total electronic energies in hartrees are given. [b] The structures are given in Figures 1 and 3 and Schemes 1 and 2. [c] Sum of energies of **T2a** and CO_2. [d] Sum of energies of **T6** and CO_2 minus the energy of H_2O. [e] One-half of the sum of B3LYP/6-31G** harmonic frequencies. [f] MP4SDQ/6-311++G** energy plus ZPE correction.

hydrogen transfer and C−C bond cleavage **T4**. This transition state is 72.8 kcal/mol higher in energy than **E1** at the MP4SDQ/6−311++G** plus ZPE level, suggesting it is a much less competitive channel to Scheme 2(c).

Starting from **E5** and following Scheme 2c, transition state searches located a structure, **T5**, for concerted hydrogen migration and C−OH_2 and C−C bond cleavage to produce CO_2, CO and H_2O. **T5** is 41.9 kcal/mol higher than **E1** at the MP4SDQ/6−311++G** plus ZPE level of theory. Extensive calculations indicate that this is perhaps the most favorable *unimolecular* decomposition pathway of oxalic acid. According to this channel, major products of thermal decomposition should be CO_2, CO, and H_2O. This prediction, however, is inconsistent with the major decomposition products, HCOOH and H_2O, observed[2] in the vapor phase decomposition at 400−430 K. To explain the observed major products, Nieminen et al.[6] suggested that unimolecular decomposition of oxalic acid follow channel 2a, but the formation of HCOOH via **T3a** might proceed on an excited state (i.e., a triplet state) which might have a smaller activation barrier. To explore feasibility of this proposal, we have optimized the equilibrium structures of DHC on the lowest triplet and the first singlet excited states by unrestricted (UHF-like) B3LYP/6-31G** method. It turns out that these equilibrium structures are 19.98 and 34.42 kcal/mol higher than **T3a** of the ground state. The transition states for hydrogen migration from oxygen to carbon on both excited state surfaces should be even higher. Therefore, in view of the low-lying transition state **T5**, unimolecular decomposition to form HCOOH and CO_2

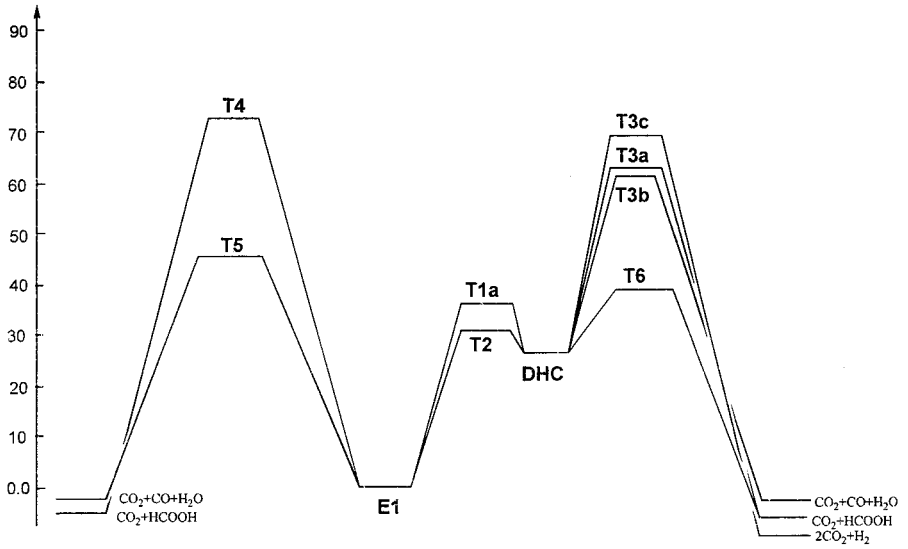

Figure 4. Schematic barrier heights of oxalic acid decomposition. The decomposition channels are depicted in Scheme 2; activation barriers are presented in Table 1.

TABLE 3: Thermodynamical Parameters of Probable Decomposition Channels on Oxalic Acid and Rate Constants Predicted by Transition State Theory

	300 (K)	325 (K)	350 (K)	375 (K)	400 (K)	425 (K)	450 (K)	475 (K)	500 (K)
E1									
S (cal K^{-1} mol^{-1})	74.07	75.83	77.55	79.22	80.83	82.40	83.93	85.42	86.87
H (hartree)	−377.45309	−377.45221	−377.45129	−377.45033	−377.44933	−377.44830	−377.44723	−377.44614	−377.44501
T5									
S (cal K^{-1} mol^{-1})	77.94	79.77	81.53	83.23	84.87	86.46	87.99	89.48	90.92
H (hartree)	−377.39188	−377.39097	−377.39002	−377.38904	−377.38803	−377.38699	−377.38592	−377.38482	−377.38370
T6									
S (cal K^{-1} mol^{-1})	75.10	76.70	78.26	79.80	81.30	82.78	84.22	85.64	87.03
H (hartree)	−377.40073	−377.39993	−377.39909	−377.39820	−377.39727	−377.39630	−377.39529	−377.39425	−377.39317
T5									
$\Delta S^{\ddagger}$ (cal K^{-1} mol^{-1})	3.88	3.94	3.98	4.02	4.04	4.05	4.06	4.06	4.05
$\Delta H^{\ddagger}$ (kcal/mol)	38.41	38.43	38.44	38.46	38.46	38.47	38.47	38.48	38.47
T6									
$\Delta S^{\ddagger}$ (cal K^{-1} mol^{-1})	1.03	0.86	0.71	0.58	0.47	0.37	0.29	0.22	0.16
$\Delta H^{\ddagger}$ (kcal/mol)	32.86	32.81	32.76	32.71	32.67	32.63	32.59	32.56	32.53
k_5 (s^{-1})	5×10^{-15}	7×10^{-13}	5×10^{-11}	2×10^{-9}	6×10^{-8}	1×10^{-6}	1×10^{-5}	2×10^{-4}	1×10^{-3}
k_6 (L mol^{-1} s^{-1})	1×10^{-9}	1×10^{-7}	5×10^{-6}	2×10^{-4}	3×10^{-3}	4×10^{-2}	4×10^{-1}	3	2×10^{1}

is definitely an unfavorable process from activation energy consideration.

Scheme 2d was proposed by Bock and Redington[8] to explain the rapid formation of HCOOH from DHC. They argued that in the reaction system there should be sufficient oxalic acid to act as the catalyst for hydrogen migration. To investigate feasibility of this proposal, we have carried out transition structure searches for a smaller model, with H_2O in the place of oxalic acid, to reduce computational cost. The optimized transition state **T6** is given in Figure 3. The relative energy of **T6** plus CO_2 calculated by MP4SDQ/6−311++G**//B3LYP/6-31G** with ZPE is 36.9 kcal/mol higher than that of **E1** plus H_2O. Thus, the calculations indicate that the decomposition channel described by Scheme 2a coupled with Scheme 2d is the lowest energy pathway generating HCOOH and CO_2. The activation energy of Scheme 2c is 5 kcal/mol higher.

3.4. Application of Transition State Theory. As the overall rate of a chemical reaction is determined by the highest activation barrier, the results presented in Table 2 suggest that reasonable thermal decomposition channels of oxalic acid be Scheme 2c and Scheme 2a coupled with Scheme 2d. The former produces CO_2, CO, and H_2O, while the latter gives CO_2 and HCOOH. The highest activation barrier along channel 2 + 2d is at **T6**, which is 5 kcal/mol lower than the activation barrier, **T5**, of channel 2c. According to transition state theory,[13] rate constant k of a chemical reaction is given by

$$k = \left(\frac{k_B T}{h}\right)\left(\frac{RT}{P^0}\right)^{m-1} e^{\Delta S^{\ddagger}/R}\, e^{-\Delta H^{\ddagger}/RT}$$

where k_B is Boltzmann's constant, h is Planck's constant, m is the order of the reaction, $\Delta S^{\ddagger}$ is activation entropy, and $\Delta H^{\ddagger}$ is activation enthalpy. The thermodynamical parameters, $\Delta S^{\ddagger}$ and $\Delta H^{\ddagger}$, can be evaluated by statistical thermodynamics from the calculated energies and vibrational frequencies of the reactants and transition states. On the basis of MP4SDQ/6-311++G**//B3LYP/6-31G** energies and the B3LYP/6-31G** force fields, the calculated thermodynamical parameters of **E1**, **T5**, and **T6** at temperatures from 300 to 500 K are given in Table 3. Rate constants calculated by the above equation with the thermodynamical parameters are also given in this table. It should be pointed out that rate constants calculated by transition state theory can only be considered qualitatively reliable and are upper limits. This is especially true for k_6 because it is the rate constant of a bimolecular reaction, which not only requires H_2O and DHC to approach each other with sufficient energy but also requires them to approach in a proper orientation. Thus, the rate constant k_6 should be smaller than predicted by the transition state theory. Table 2 shows qualitatively that at low temperatures ($T < 400$ K); both reaction channels are slow and the bimolecular channel dominates (as k_6 is significantly larger than k_5). With increasing temperature, k_5 increases its magnitude more rapidly than k_6 does. Even though k_5 is still several orders of magnitude smaller than k_6 at 500 K, the rates of reactions of

these two channels may not differ so much because channel 2a + 2d is bimolecular at **T6** and the rate is equal to k_6[DHC][oxalic acid], while the rate of channel 2c is equal to k_5[oxalic acid]. Because DHC is a radical, its concentration should be much lower than oxalic acid; therefore, the rate for channel 2a +2d should be much lower than it appears to be from inspecting the rate constant.

Experimentally, most of the gas phase kinetics studies[2] of oxalic acid decomposition were carried out at temperatures above 100 °C (373 K). This is in line with the calculated results, because at temperatures lower than 400 K, the rate constants are too small, and therefore, the decomposition is too slow. In the temperature range from 127 to 180 °C, it was found experimentally[2] that the kinetic carbon isotope effect of oxalic acid decomposition is strongly temperature dependent and it reverses at about 145 °C. The large temperature dependence and reversal of kinetic isotope effect were suggested to arise in the accessibility to reaction of more than one reaction channel, not in isotope differential effects themselves.[2] The calculated results seem to support this proposal and indicate that at high temperatures decomposition through channel 2c might become competitive to decomposition through channel 2a + 2d.

4. Conclusions

This study shows that density functional theory B3LYP/6-31G** structures and relative energies of the rotational isomers of oxalic acid are very similar to the much more expensive MP2/6-31G** results. It is confirmed that the most stable conformer of oxalic acid is the doubly hydrogen-bonded C_{2h} structure and that there are four other planar conformers within 6 kcal/mol. It is predicted that unimolecular formation of carbon dioxide and dihydroxylcarbene (DHC) from oxalic acid is a feasible thermal process, but unimolecular formation of HCOOH from DHC has an activation barrier that is much higher than unimolecular formation of CO_2, CO, and H_2O from oxalic acid via a concerted transition state. On the other hand, hydrogen migration from oxygen to carbon of DHC to produce HCOOH can be accomplished through a hydrogen exchange with H_2O (a model for oxalic acid) with an activation barrier lower than all unimolecular decomposition channels considered. Transition state theory calculations indicate that this bimolecular channel might be responsible for the rapid formation of CO_2 and HCOOH in gas phase oxalic acid decomposition, thus confirming the proposal of Bock and Redington. With increasing temperature the unimolecular channel to produce CO_2, CO, and H_2O might become significant and it seems to support the experimental suggestion that the observed large temperature dependence and reversal of kinetic isotope effect arise in the accessibility to reaction of more than one reaction channel, not in isotope differential effects themselves. It should be noted that the observed rapid formation of HCOO H and CO_2 might also proceed via a heterogeneous reaction at the walls of the container, therefore a bimolecular route in the gas phase represents only one of the possibilities.

Acknowledgment. This study was partially supported by the Research Development Committee of East Tennessee State University and by a Cottrell College Science award of Research Corporation.

References and Notes

(1) Wobbe, D. E.; Noyes, W. A., Jr. *J. Am. Chem. Soc*. **1926**, *48*, 2856.
(2) Lapidus, G.; Barton, D.; Yankwich, P. E. *J. Phys. Chem*. **1964**, *68*, 1863; *Ibid.* **1966**, *69*, 407; *Ibid.* **1966**, *70*, 1575; *Ibid.* **1966**, *70*, 3135.
(3) Clark, L. W. *J. Am. Chem. Soc.* **1955**, *77*, 6191; Clark, L. W. *J. Phys. Chem.* **1957**, *61*, 699. *Ibid.* **1958**, *62*, 633. *Ibid.* **1963**, *67*, 1355. *Ibid.* **1966**, *70*, 1597.
(4) Yamamoto, S.; Back, R. A. *J. Phys. Chem*. **1985**, *89*, 622.
(5) Kakumoto, T.; Saito, K.; Imamura, A. *J. Phys. Chem*. **1987**, *91*, 2366.
(6) Nieminen, J.; Rasanen, M.; Murto, J. *J. Phys. Chem.* **1992**, *96*, 5303.
(7) Van Alsenoy, C.; Klimkowski, V. T.; Schafer, L. *J. Mol. Struct. (THEOCHEM)* **1984**, *109*, 321.
(8) Bock, C. W.; Redington, R. L. *J. Chem. Phys.* **1986**, *85*, 5391.
(9) Becke, A. D. *J. Chem. Phys.* **1993**, *98*, 5648.
(10) Lee, C.; Yang, W.; Parr, R. G. *Phys. Rev.* **1988**, *B37*, 785. Miehlich, B.; Savin, A.; Stoll, H.; Preuss, H. *Chem. Phys. Lett*. **1989**, *157*, 200.
(11) Frisch, M. J.; Trucks, G. W.; Schlegel, H. B.; Gill, P. M. W.; Johnson, B. G.; Robb, M. A.; Cheeseman, J. R.; Keith, T.; Petersson, G. A.; Montgomery, J. A.; Raghavachari, K.; Al-Laham, M. A.; Zakrzewski, V. G.; Ortiz, J. V.; Foresman, J. B.; Cioslowski, J.; Stefanov, B. B.; Nanayakkara, A.; Challacombe, M.; Peng, C. Y.; Ayala, P. Y.; Chen, W.; Wong, M. W.; Andres, J. L.; Replogle, E. S.; Gomperts, R.; Martin, R. L.; Fox, D. J.; Binkley, J. S.; Defrees, D. J.; Baker, J.; Stewart, J. P.; Head-Gordon, M.; Gonzalez, C.; Pople, J. A. *Gaussian 94*, Revision B.1; Gaussian, Inc.: Pittsburgh, PA, 1995.
(12) Gonzalez, C.; Schlegel, H. B. *J. Chem. Phys.* **1989**, *90*, 2154. Gonzalez, C.; Schlegel, H. B. *J. Phys. Chem.* **1990**, *94*, 5523.
(13) Eyring, H. *J. Chem. Phys.* **1935**, *3*, 107. Evans, M. G.; Polanyi, M. *Trans. Faraday Soc*. **1935**, *31*, 875.
(14) Nahlovska, Z.; Nahlovsky, B.; Strand, T. G. *Acta Chem. Scand*. **1970**, *24*, 2617.
(15) Redington, R. L.; Redington, T. E. *J. Mol. Struct. (THEOCHEM)* **1978**, *48*. 165.
(16) Scott, A. P.; Radom, L. *J. Phys. Chem*. **1996**, *100*, 16502.
(17) Stace, B. C.; Oralratmanee, C. *J. Mol. Struct*. (THEOCHEM) **1973**, *18*, 339.